Ligand-induced Protease Receptor Translocation into Caveolae: A Mechanism for Regulating Cell Surface Proteolysis of the Tissue Factor–dependent Coagulation Pathway

Joel R. Sevinsky,* L. Vijay Mohan Rao,‡ and Wolfram Ruf*

*Departments of Immunology and Vascular Biology, The Scripps Research Institute, La Jolla, California 92037; and ‡Department of Biochemistry, The University of Texas Health Center at Tyler, Tyler, Texas 75710

Abstract. The ability to regulate proteolytic functions is critical to cell biology. We describe events that regulate the initiation of the coagulation cascade on endothelial cell surfaces. The transmembrane protease receptor tissue factor (TF) triggers coagulation by forming an enzymatic complex with the serine protease factor VIIa (VIIa) that activates substrate factor X to the protease factor Xa (Xa). Feedback inhibition of the TF·VIIa enzymatic complex is achieved by the formation of a quaternary complex of TF·VIIa, Xa, and the Kunitz-type inhibitor tissue factor pathway inhibitor (TFPI). Concomitant with the downregulation of TF·VIIa function on endothelial cells, we demonstrate by immunogold EM that TF redistributes to caveolae. Consistently, TF translocates from the Triton X-100–soluble membrane fractions to low-density, detergent-insoluble microdomains that inefficiently support TF·VIIa proteolytic function. Downregulation of TF·VIIa function is dependent on quaternary complex formation with TFPI that is detected predominantly in detergent-insoluble microdomains. Partitioning of TFPI into low-density fractions results from the association of the inhibitor with glycosyl phosphatidylinositol–anchored binding sites on external membranes. Free Xa is not efficiently bound by cell-associated TFPI; hence, we propose that the transient ternary complex of TF·VIIa with Xa supports translocation and assembly with TFPI in glycosphingolipid-rich microdomains. The redistribution of TF provides evidence for an assembly-dependent translocation of the inhibited TF initiation complex into caveolae, thus implicating caveolae in the regulation of cell surface proteolytic activity.

CELLS accomplish tasks of invasion, migration, tissue remodeling and cell–cell communication in part through the regulated expression of cell-associated protease systems. Cell surface protease cascades are triggered by the upregulation of protease receptors, such as the urokinase receptor of the fibrinolytic system (14) and tissue factor (TF)[1] that initiates the plasma coagulation pathways (48). Based on structural homology in the extracellular domain, TF is classified as a member of the cytokine receptor family and most closely related to the interferon and IL-10 receptors (48). However, in contrast to the four helix bundle ligands of the latter, TF binds the multidomain serine protease factor VIIa (VIIa) with subnanomolar affinity. The assembly of the protease into the TF·VIIa complex results in markedly enhanced proteolytic activation of the substrates factor X and factor IX. The product protease factor Xa (Xa) activates prothrombin to thrombin that converts fibrinogen into an adhesive fibrin matrix as well as elicits diverse cellular responses through the signaling thrombin receptor (63).

The TF-driven coagulation pathway is regulated by specific inhibitors, i.e., the serine protease inhibitor (serpin) antithrombin III and the Kunitz-type inhibitor tissue factor pathway inhibitor (TFPI) (6, 41). Both inhibitors are present in plasma, but the latter is also found on endothelial cells, the major biosynthetic source for TFPI (1). TFPI inhibits the TF·VIIa complex most efficiently in the presence of Xa (7). The second Kunitz-type domain of TFPI binds and inhibits Xa, and complex formation of TFPI with Xa is thought to facilitate the assembly of the first Kunitz-type domain with VIIa when bound to TF (6). This results in a stable quaternary complex characterized by slow dissociation. The third Kunitz-domain and the basic carboxyl terminus of TFPI are implicated in the binding of glycosaminoglycans (15, 66), which are inferred to be expressed on vascular endothelial cells (53). The binding site and the cellular localization of TFPI on endothelial cells are not established.

Address all correspondence to Wolfram Ruf, Department of Immunology, IMM-17, The Scripps Research Institute, 10666 North Torrey Pines Road, La Jolla, CA 92037. Tel.: (619) 554-2748. Fax: (619) 554-6146.

1. *Abbreviations used in this paper*: EGR-Xa, factor Xa inhibited by glutamyl-glycyl-arginyl-chloromethyl ketone; GPI, glycosyl phosphatidylinositol; LDL, low density lipoprotein; TF, tissue factor; TFPI, TF pathway inhibitor; TNFα, tumor necrosis factor α; VIIa, factor VIIa; Xa, factor Xa.

Endothelial cells in primary culture do not express TF unless stimulated by cytokines, such as tumor necrosis factor α (TNFα) (37). In most cell types, TF is predominantly expressed on the cell surface and accessible to functional inhibition by mAbs (12). Expression of TF was observed on the basolateral side of endothelial cells after stimulation in vitro (33); this pattern is consistent with expression of TF on cellular processes or membrane ruffles documented for fibroblasts (8), certain tumor cells (34), and macrophages (22). Other studies documented expression of TF predominantly on the apical side of endothelial cells (25, 35), and this restricted display was attributed to the formation of tight junctions between endothelial cells in the monolayer (35). Endothelial cell expression of TF in vivo was demonstrated in the spleen of septic animals (13) and in the tumor vasculature (11). Regulation of TF function is thus considered critical to maintain the anticoagulant properties of the vascular endothelium in vivo.

We here characterize the regulation of cell surface proteolytic function of the TF·VIIa complex on endothelial cells and find that the downregulation of TF function is accompanied by a translocation of TF into noncoated plasmalemma vesicles (caveolae). Caveolae are morphologically defined small plasmalemma vesicles characterized by the presence of the marker protein caveolin, a structural component of the vesicles (44). Caveolae have a membrane composition that is rich in glycosphingolipids and cholesterol, resulting in decreased solubility in certain detergents. Caveolae were first described as a transport system mediating transcytosis across endothelial cells (38, 55) and play a role in the uptake (potocytosis) of certain small molecules that is mediated by glycosyl phosphatidylinositol (GPI)–linked receptors (2). Molecules involved in the signal transduction pathways have been shown to be enriched in glycosphingolipid-rich microdomains of cellular membranes, further suggesting a regulatory role of caveolae in signal transduction (17, 54). In this study, we demonstrate that downregulation of TF-initiated proteolytic function is associated with receptor translocation into caveolae. This inhibition of TF function is mediated by cell-associated TFPI, and we elucidate critical interactions that are required for assembly of the TF·VIIa complex with TFPI. This study provides insight into the control of cellular proteolytic functions that is mediated by the redistribution of the inhibited TF·VIIa initiation complex to caveolae.

Materials and Methods

Reagents

The mAbs to TF factor X and VIIa had been characterized and were purified from ascites on immobilized protein A as described (50). Polyclonal antibodies to TFPI were generated in rabbits and purified as described (64), and mAbs to the first (4903) or second (4904) Kunitz domain of TFPI were purchased from American Diagnostica Inc. (Greenwich, CT). The mAb to caveolin (anti–22-kD Rous Sarcoma Virus-Src substrate) was obtained from ICN Biomedicals Inc. (Irvine, CA). HRP-conjugated secondary antibodies and reagents for chemiluminescence detection were from Amersham Life Science (Arlington Heights, IL). Secondary gold-conjugated antibodies were from BBI International (Cardiff, UK). Recombinant VIIa was expressed in CHO cells and purified as described (46). Factor X was purified from plasma as described (49). Human Xa inactivated with glutamyl-glycyl-arginyl-chloromethyl ketone (EGR-Xa) and unmodified Xa were purchased from Haematologic Technologies Inc. (Essex Junction, VT).

Cell Culture

The spontaneously transformed human umbilical vein endothelial cell line ECV304 was obtained from the American Type Culture Collection (Rockville, MD) (ATCC CRL-1998) and was grown as monolayer in media 199 supplemented with 10% FBS and 2 mM glutamine. Before all experiments, confluent ECV304 cell monolayers were stimulated for 5 h with 10 ng/ml recombinant TNFα (Cetus Corp., Emeryville, CA) to induce maximal TF expression. Stimulation with TNFα consistently resulted in an increased expression of TF based on immunochemical detection by Western blot analysis of fracionated cell lysates or by quantitative immunoassay of whole cell lysates (see below). All incubations and washes were carried out in cell buffer (21 mM Hepes, 137 mM NaCl, 5 mM KCl, 0.75 mM Na_2HPO_4, 5.5 mM glucose, 2 mM $CaCl_2$, pH 7.4), unless otherwise noted.

ELISA

TF concentration of ECV304 cells was determined by an mAb-based sandwich ELISA, as described previously in detail (52). Cells were lysed in 6 mM CHAPS before dilution in assay buffer. The capture antibody was TF9-6B4, and the detection antibody was biotinylated TF8-5G9. These mAbs are directed to nonoverlapping epitopes on TF (50). Bound secondary antibody was detected using streptavidin-conjugated HRP and tetramethylbenzidine as substrate. The concentration of TFPI in ECV304 lysates was determined by a commercially available immunoassay that is based on a polyclonal capture antibody and a monoclonal detection antibody (IMUBIND Total TFPI ELISA Kit; American Diagnostica Inc.). Cell pellets were lysed in 50 mM CHAPS and serially diluted in the sample dilution buffer recommended by the manufacturer. Mean and SD were calculated for cell pellets that were harvested on different occasions.

Determination of TFPI Concentration by Functional Assay

Cells were lysed in 15 mM octylglucopyranoside and diluted fivefold in buffer containing 5 mM octylglucopyranoside. TFPI activity was measured in a two-stage end-point chromogenic assay. First, test samples were incubated with a reaction mixture containing a limited concentration of VIIa (0.5 ng/ml), relipidated TF (10 ng/ml), Xa (5 ng/ml), and $CaCl_2$ (10 mM) in 60 μl for 30 min at room temperature. Then, 100 μl of a mixture of factor X (2.5 μg/ml), $CaCl_2$, and Chromozym X (1.25 mg/ml) was added to the reaction. After 20 min, absorbance at 405 nm was measured. The concentrations of TFPI in the samples were calculated from a standard curve of purified recombinant TFPI diluted in 5 mM octylglucopyranoside.

Assay for Cell Surface Proteolytic Activity of TF·VIIa

Stimulated ECV304 cells in 24-well tissue-culture plates were washed and incubated with 10 nM VIIa in cell buffer for 60 min at 4°C. Dose titration of VIIa in preliminary experiments established that this concentration of VIIa was sufficient to saturate TF on stimulated ECV304, consistent with the findings on other cell types (29). After washes in cell buffer (see above), cells were warmed to 37°C for 10 min before the addition of 5 μM substrate factor X (in a total volume of 0.5 ml). Samples (50 μl) were taken during a 30-min incubation time and quenched in 150 μl of 100 mM EDTA. The amount of Xa generated at each time was determined from the hydrolysis of the chromogenic substrate Spectrozyme FXa (American Diagnostica Inc.) added to the quenched reaction (52). Rates of Xa generation were calculated from the increase in product between two consecutive time points. In antibody blocking experiments, 100 μg/ml polyclonal anti-TFPI IgG was included in the preincubation with VIIa (5 nM) at 37°C for 30 min followed by the addition of substrate factor X (500 nM) (all concentrations are based on the final reaction volume). Samples were taken as above for determination of the rate of Xa generation.

Electron Microscopy

After experimental treatment and antibody staining, cells were fixed in modified Karnovsky's fixative (2% paraformaldehyde, 1.5% glutaraldehyde in 0.1 M cacodylate buffer, pH 7.4) for 1–2 h at 4°C and postfixed in 1% OsO_4 for 1 h at room temperature. The fixed cells were stained (en block) in 1% aqueous uranyl acetate, dehydrated in graded ethanol, and embedded in TAAB 812 epoxy resin (TAAB Laboratories Equipment, Reading, Berks, UK). Thin sections were cut parallel to the dish to yield an en face view. For the purpose of counting gold granules on vertical sections, two pieces of cell-bearing epon sheets were sandwiched, with cell

sides facing each other and reembedded to yield two lines of perpendicularly sectioned cells. These sections were mounted on a Pelco 100-bar grid with 285-μm intervals (Ted Pella, Inc., Irvine, CA). Thin sections were stained in uranyl acetate and lead citrate and viewed with an electron microscope (HU 12A; Hitachi Ltd., Tokyo, Japan).

The conditions for the specific experiments were as follows: (*a*) localization of TF by indirect immunogold detection: stimulated ECV304 cells were washed and incubated with 30 μg/ml TF9-10H10 IgG with or without 5 nM VIIa and 200 nM factor X for 30 min at 37°C. Cells were then washed and incubated with goat anti–mouse IgG 10-nm gold conjugate for 30 min at 4°C followed by washes before fixation. (*b*) Quantitation of TF translocation with directly labeled anti-TF Fab fragments: Fab fragments of TF9-10H10 were generated by papain digestion of IgG and monovalent protein was purified to homogeneity by ion exchange chromatography as described (51). A gold colloid with an average size of <5 nm was produced by the reduction of tetrachloroauric acid with sodium borohydrid (62). To 50 ml of 0.01% chloroauric acid, a freshly prepared 0.1 M sodium borohydrid solution was added drop by drop in a rapid succession until the color turned reddish orange. The colloidal gold particles were complexed with TF9-10H10 Fab in deionized water according to the method of Geoghegan and Ackerman (19). Stimulated ECV304 cells were washed and incubated with TF9-10H10 Fab gold conjugate (30 μg/ml) without (control) or with 10 nM VIIa for 1 h at 4°C. Cells were washed rapidly three times and incubated without (control) or with 200 nM factor X for 15 min at 37°C. After rapid washes with ice-cold buffer, cells were immediately fixed at 4°C.

Separation of Trition X-100–insoluble Complexes by Sucrose Gradient Ultracentrifugation

The protocol described by Lisanti et al. (31) was used with the following specific experimental conditions: ECV304 cells were grown to confluence for 3 d in 150-cm^2 flasks and stimulated for 5 h with TNFα. Cells were washed and incubated with or without 5 nM VIIa in cell buffer for 1 h at 4°C. For blocking experiments, inhibitory polyclonal anti-TFPI antibody was included at 30 μg/ml during this preincubation step. The supernatant was removed, and the cells were incubated for an additional 15 min at 37°C with cell buffer alone or cell buffer containing either 200 nM factor X, 5 nM Xa, or 5 nM EGR-Xa. For the blocking experiment with anti-TFPI antibody, 200 nM factor X and 30 μg/ml polyclonal anti-TFPI were included during the latter incubation. Cells were then washed with ice-cold cell buffer followed by cell buffer with lower $CaCl_2$ (0.5 mM) to reduce the amount of proteins (VIIa, factor X, Xa) that were nonspecifically associated with cell membranes through their γ-carboxyglutamic acid–rich domains. All subsequent steps were carried out at 4°C. The cells were harvested by scraping in low $CaCl_2$ cell buffer, and a cell pellet was obtained by centrifugation at 200 *g*. The pellet was resuspended in 2 ml of MES-buffered saline (25 mM MES, 150 mM NaCl, pH 6.5) containing 1% Triton X-100, 1 mM $NaVO_4$, 1 mM PMSF, and 100 μM $CaCl_2$. Cells were homogenized with 10 strokes in a loose-fitting dounce homogenizer, and then sucrose was added to 40%. Homogenates were placed at the bottom of an ultracentrifuge tube, and a 30–5% sucrose gradient in MES-buffered saline containing 1 mM $NaVO_4$, 1 mM PMSF, and 100 μM $CaCl_2$, but no Triton X-100, was placed on top. The gradient was centrifuged at 39,000 rpm in a rotor (SW40Ti; Beckman Instruments, Fullerton, CA) for 16–20 h at 4°C. Gradients were collected in eight 1.5-ml fractions from the top. Fractions 1–6 contain material floating in the sucrose gradient, whereas fraction 7 included the 30/40% sucrose interface, and fraction 8 contained the remaining Triton X-100–soluble material in 40% sucrose. The protein concentration of each fraction was determined by bicinchoninic acid assay (Pierce Chemical Co., Rockford, IL).

Western Blot Analysis and Quantitation of the Cellular Distribution of TF

Fractions collected from the sucrose gradient were diluted twofold in Triton X-100–free MES-buffered saline before precipitation with 10% TCA. The precipitates were solubilized in nonreducing SDS-PAGE sample buffer at a concentration of 1 mg/ml. A constant amount of protein (5 μg) was separated on 8–16% gradient gels followed by transfer onto Immobilon P (Millipore Corp., Bedford, MA) using a semidry transblot system and buffers according to Kyhse-Anderson (28). TF was detected with polyclonal goat anti-TF IgG that had been affinity purified on immobilized TF extracellular domain (50). VIIa was detected with mAb F5-13B12 and factor X/Xa with mAb F21-4.2, both of which were generated in the laboratory by standard hybridoma technology and which have been screened for specific reactivity with purified vitamin K–dependent proteins. TFPI was detected by polyclonal rabbit anti-TFPI IgG. Caveolin was detected by mAb (anti–22-kD Rous Sarcoma Virus-Src substrate). Bound primary antibody was detected by appropriate HRP-conjugated secondary antibody that was visualized using chemiluminescence reagents from Amersham Corp. and exposure of X-Omat AR film (Eastman-Kodak Co., Rochester, NY). To quantify the cellular distribution of TF or TFPI, a defined amount of purified TF or TFPI was loaded on each gel and transferred to membranes that were used for Western blotting. The quantitation was based on densitometric analysis of the films using a densitometer and ImageQuant software (Molecular Dynamics, Sunnyvale, CA).

Determination of TF Functional Activity in Gradient Fractions

Fractions were diluted in 25 mM MES, 150 mM NaCl, pH 6.5, to give a final concentration of 2.5 μg/ml of total protein in the assay. TF in the fractions was assembled with 10 nM VIIa and 200 nM factor X at a final $CaCl_2$ concentration of 2 mM at 37°C. The reaction was quenched with 50 mM EDTA after 5–30 min, and product Xa generation was determined with chromogenic substrate. TF-dependent generation of Xa was assured by control reactions that included 1 mg/ml of the inhibitory anti-TF mAb TF9-6B4 that blocks TF function by >90% at the given concentration (47). To block TFPI function in the fractions, the diluted fractions were preincubated with 50 μg/ml polyclonal anti-TFPI antibody for 15 min at 37°C before the addition of VIIa and factor X.

Protease Treatment and Trion X-114 Fractionation of ECV304 Cells

ECV304 that were grown to confluence for 3 d were detached with 5 mM EDTA, washed once in cell buffer, and counted. Cells were >90% viable. 3×10^6 cells were incubated in 0.5 ml cell buffer containing 0.1% NaN_3 without or with proteases (proteinase K, chymotrypsin, or elastase) at 500 μg/ml for 2 h on ice. After four washes with ice-cold 100 mM Tris, 1 mM EDTA, 2000 U/ml aprotinin, 100 μM PMSF, pH 8.1, cells were pelleted for ELISA or fractionated with Triton X-114. Enzymatic cleavage of the GPI linkage with 0.5 U of phospholipase C (Boehringer Mannheim Biochemicals, Indianapolis, IN) was carried out in cell buffer for 15 min at 37°C, followed by one wash with cold wash buffer as above before pelleting of the cells. Cell pellets were lysed in 1 ml of 1% Triton X-114 in 0.1 M Tris, 10 mM EDTA, 2000 U/ml aprotinin, and 100 μM PMSF by incubating with repeated mixing on ice for 15 min (3). Debris was removed by centrifugation at 14,000 *g* at 4°C. Phase separation was induced by incubation of the cleared detergent lysate for 5 min at 37°C, followed by brief centrifugation at 14,000 *g* to separate detergent and aqueous phase. The same buffer lacking detergent was added, and the extraction was repeated once. The detergent pellicle was extracted with acetone, resulting in precipitation of the solubilized protein that was resuspended in nonreducing sample buffer. Extracted proteins from 5×10^5 cells were loaded per lane for electrophoresis, transfer, and Western blotting using polyclonal anti-TFPI antibody as described above.

Results

Downregulation of TF·VIIa Complex Function on Endothelial Cells

Human endothelial cells in culture express TF in response to stimulation with TNFα (37). We observed that the spontaneously transformed human endothelial cell line ECV304 (61) can be induced to express TF after stimulation with TNFα, thus providing an abundant cell source for studying the regulation of TF function on endothelial cells. By ELISA, we determined that unstimulated ECV304 express 42,700 ± 14,200 molecules ($n = 3$) of TF per cell and that the number increases to 128,000 ± 6,000 ($n = 3$) on TNFα-stimulated cells. Preincubation of intact ECV304 cells with inhibitory anti-TF mAbs before cell lysis blocked >95% of TF function, confirming that TF is almost exclusively ex-

pressed on the cell surface, as observed for other cell types (12). In the experiments described, ECV304 cells were stimulated for 5 h with 10 ng/ml TNFα, and cell surface–expressed TF was saturated with the ligand VIIa (10 nM) by incubation for an additional hour at 4°C. Unbound VIIa was removed by washes with Ca^{2+}-containing buffer at 37°C, and factor X was added at the same temperature to monitor proteolytic function of the TF·VIIa complexes expressed on the cell surface.

The rate of factor X activation progressively declined with time (Fig. 1), and a 35–60% reduction was consistently observed in all experiments after a 15-min reaction. TF·VIIa function consistently declined to <50% after 30 min, but >80% inhibition, as shown in Fig. 1, was not observed in all experiments. The decrease of function is not attributable to substrate depletion, because <1% of the initially present substrate was used after 30 min. The downregulation of TF·VIIa function was dependent on the presence of substrate, since preincubation in buffer for 30 min before addition of substrate resulted in identical initial rates and a similar decrease in function over time (Fig. 1). This finding excludes the interpretation that the loss of cell surface TF·VIIa function is a consequence of dissociation or internalization of the complex that may occur independent of substrate.

In control experiments, cells were metabolically inhibited with 0.1% NaN_3 to evaluate the energy dependence of the observed reduction in TF·VIIa function. There was no difference between metabolically active and inhibited cells, indicating that the inhibition of function is independent of an energy producing metabolism. TF·VIIa on endothelial cells has been shown to activate the substrate factor IX (4). To test whether the decrease in TF·VIIa function follows interaction with any substrate, ECV304 were incubated with the substrate factor IX (300 nM) for 30 min, followed by rapid washes to remove product IXa and remaining substrate factor IX. Factor X was then added to determine TF·VIIa functional activity of the pretreated cells. Preincubation with factor IX neither decreased the initial rate of factor X activation nor the subsequent decrease in TF·VIIa proteolytic function (data not shown). Thus, substrate interaction per se is not sufficient to reduce TF·VIIa complex function. These data are consistent with inhibition of TF·VIIa function specifically dependent on the conversion of factor X to the product Xa.

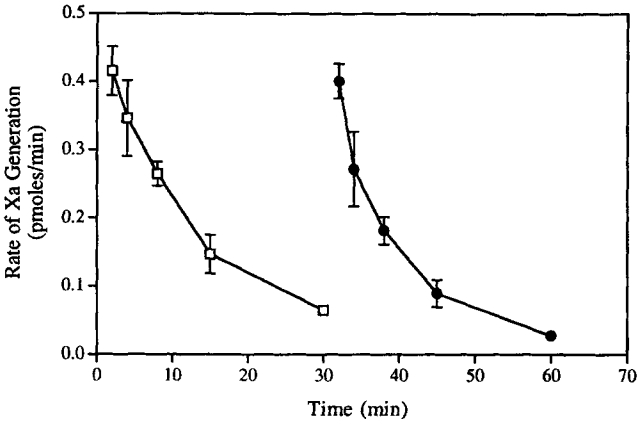

Figure 1. Downregulation of TF·VIIa proteolytic function on endothelial cells. TNFα-stimulated ECV304 cells were preincubated with 10 nM VIIa to form the TF·VIIa complex and washed. Substrate factor X (5 μM) was added, and the rate of Xa generation was determined as a measure for proteolytic function of TF·VIIa. Proteolytic function was rapidly downregulated (□). Preincubation of the cells in buffer for 30 min before the addition of substrate did not change the initial rate or downregulation of TF·VIIa function (●). Mean and SD of triplicate determinations are shown.

Ultrastructural Localization of TF

To gain insight into the cellular events associated with the downregulation of cell surface TF·VIIa complex function, we investigated the cellular distribution of TF by immunogold EM. To tag TF, we used a noninhibitory anti-TF mAb (TF9-10H10) (50), which neither inhibits VIIa binding to TF nor the subsequent assembly of substrate and of inhibitors with the TF·VIIa complex. This functionally neutral antibody specifically reacts with TF on cells, based on analysis by immunofluorescence microscopy demonstrating blocking of the staining by addition of a fivefold molar excess of recombinant soluble TF extracellular domain (49). In initial experiments, cells were tagged with TF9-10H10 IgG and incubated at 37°C in the absence (control) or presence of VIIa and substrate factor X for 30 min. After transfer onto ice, the mAb specifically bound to TF was reacted with 10-nm gold–conjugated anti–mouse antibody followed by fixation for transmission EM. In control reactions, TF was predominantly detected on the cell membrane and on cellular processes. In the presence of VIIa and factor X, gold particles were found more frequently in noncoated plasmalemma vesicles with morphological appearance and size consistent with caveolae (Fig. 2 *a*), while some TF was still found in both the cell membrane and cellular processes.

To rule out the possibility of nonspecific clustering due to secondary antibody cross-linking, monovalent Fab fragments of TF9-10H10 (51) were generated and conjugated to small (<5 nm) gold particles. TF tagged with directly labeled Fab fragments was also found more frequently in caveolae when VIIa and factor X were added. Vertical thin sections were analyzed to quantify the cellular distribution of TF. The basal and apical contours of nucleated sections were examined, and the number of gold particles were counted. Fig. 2 illustrates the locations in which gold particles were detected. The most frequent location was the smooth cell membrane (Fig. 2 *e*) where clusters of one to ten particles were detected. Clusters of one to three particles were found on cellular processes (Fig. 2 *b*), and in caveolae clusters of one to five gold particles were detected (Fig. 2, *d* and *e*). Gold particles were typically absent from clathrin-coated pits that were identified by the characteristic coat (Fig. 2 *c*). A total of 41 sections were analyzed for the control and the experimental group, both of which had similar numbers of caveolae and clathrin-coated pits (Table I). Whereas <4% of the gold particles on the control were found in caveolae, the localization of TF in caveolae was increased to 34% in the presence of VIIa and factor X. This percentage of gold particles in caveolae was consistently obtained by two investigators who analyzed the sections according to the given criteria. These

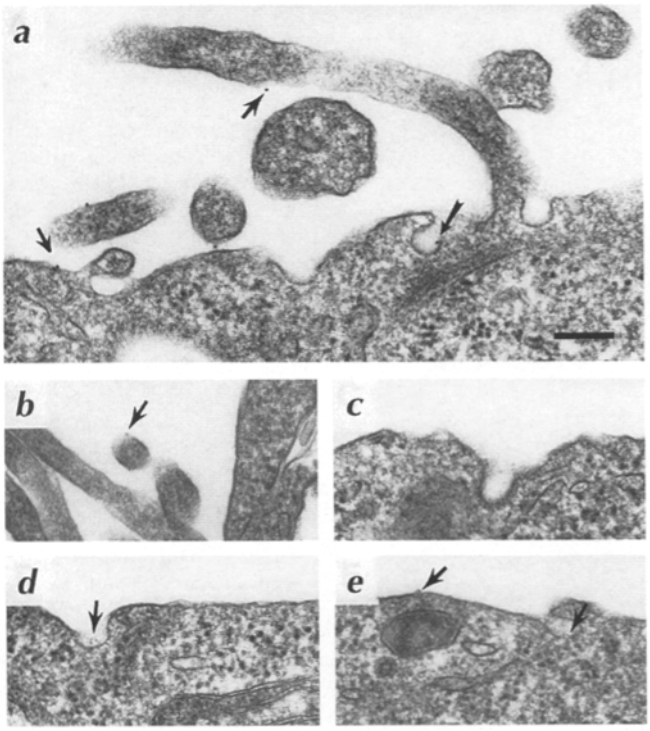

Figure 2. Ultrastructural localization of TF by immunogold EM. TNFα-stimulated ECV304 were incubated with VIIa and factor X, and TF was tagged by a noninhibitory mAb (TF9-10H10). (*a*) Indirect detection of TF using 10-nm gold–conjugated anti–mouse secondary antibody. TF was localized on the cell membrane (*left*), on cellular processes (*middle*), and in caveolae (*right*). (*b–e*) TF was directly detected with <5 nm gold conjugated to monovalent Fab fragments of TF9-10H10. Typical localization of TF on processes (*b*), the cell membrane (*e*, *left*), and caveolae (*d* and *e*, *right*) is shown. TF was usually absent from clathrin-coated pits (*c*). Bar, 200 nm.

data are consistent with the increased localization of TF in caveolae suggested by indirect detection of the tagging antibody.

Changes of Triton X-100 Solubility of TF in the Presence of Substrate

Solubilization of endothelial cells with Triton X-100 followed by sucrose gradient centrifugation has been used to isolate cellular fractions that are highly enriched in caveolin and vesicular structures resembling caveolae (31). We examined whether the interaction of factor X with the TF·VIIa complex changed the detergent solubility of TF that would be expected from a translocation into glycosphingolipid-rich microdomains on the cell surface. ECV304 cells were lysed in Triton X-100 and fractionated on a 5–30% sucrose gradient by ultracentrifugation (31). Fractions (1.5 ml) were collected from the top of the gradient and analyzed by Western blotting for TF. In controls, TF was mostly found in the detergent soluble fractions 7 and 8 that had been adjusted to 40% sucrose (Fig. 3). In cells that had been incubated with VIIa and factor X, TF translocated to Triton X-100–insoluble fractions floating at ~14–25% sucrose. Based on laser densitometry, the concentration of TF in the detergent-insoluble fractions increased 10-fold

Table I. Quantitation of the Cellular Distribution of TF by Immunogold EM

	Control	VIIa and factor X added
Number of sections* analyzed	41	41
Average number of caveolae per section	5.9	4.8
Average number of coated pits per section	0.9	1.1
Gold particles		
Total	342	237
On cell surface	268 (78%)	121 (51%)
On cellular processes	61 (18%)	34 (14%)
In caveolae	13 (4%)	81 (34%)
In clathrin-coated pits	0 (0%)	1 (1%)

*Vertical nucleated sections of ECV304.

after addition of VIIa and factor X. This represents a redistribution of TF, because the total cellular TF, as determined from densitometric quantitations, did not change significantly (total TF for separations with no translocation: 29 ± 11 ng [n = 6]; with translocation: 36 ± 22 ng [n = 4]). The low density fractions 3–5 contained caveolin that was not detected in the detergent-soluble material. TF thus translocates into fractions that contain essentially all the cellular caveolin, consistent with the ultrastructural localization of TF in caveolae. The Triton X-100–insoluble fractions also contained VIIa, demonstrating that the TF·VIIa complex did not dissociate during translocation (Fig. 3). We further detected Xa as a double band, but not the zymogen precursor factor X that can be distinguished by its larger size under nonreducing conditions. This indicates that Xa translocated with TF·VIIa into caveolae.

Blocking TFPI Abolishes Downregulation of TF Function

One of the major mechanisms regulating proteolytic function is inhibition by specific inhibitors. The TF·VIIa complex is inhibited by TFPI, a Kunitz-type inhibitor that is known to be expressed by endothelial cells (1). By antibody inhibition, we tested whether TFPI may be involved in the downregulation of TF function on ECV304 cells. In the presence of polyclonal anti-TFPI antibodies, the initial rates of factor X activation were increased as compared to the noninhibited control (Fig. 4). The lower rate in the latter case may reflect an initial rapid downregulation by TFPI during the 2-min sampling period that was used to determine the intial rates for the reaction. Notably, the rates of factor X activation in the presence of anti-TFPI antibodies did not decrease significantly over the entire 30-min reaction period (Fig. 4). mAbs to the first or second Kunitz-type domain of TFPI similarly prevented inhibition of TF·VIIa function. Inhibition of TF·VIIa by TFPI thus appears to be responsible for the downregulation of TF-dependent proteolytic function.

Translocation of TF·VIIa Results in the Inhibition of Function

Since the translocation event paralleled the downregulation of TF function, we investigated whether TF was functional in both the detergent-insoluble and -soluble frac-

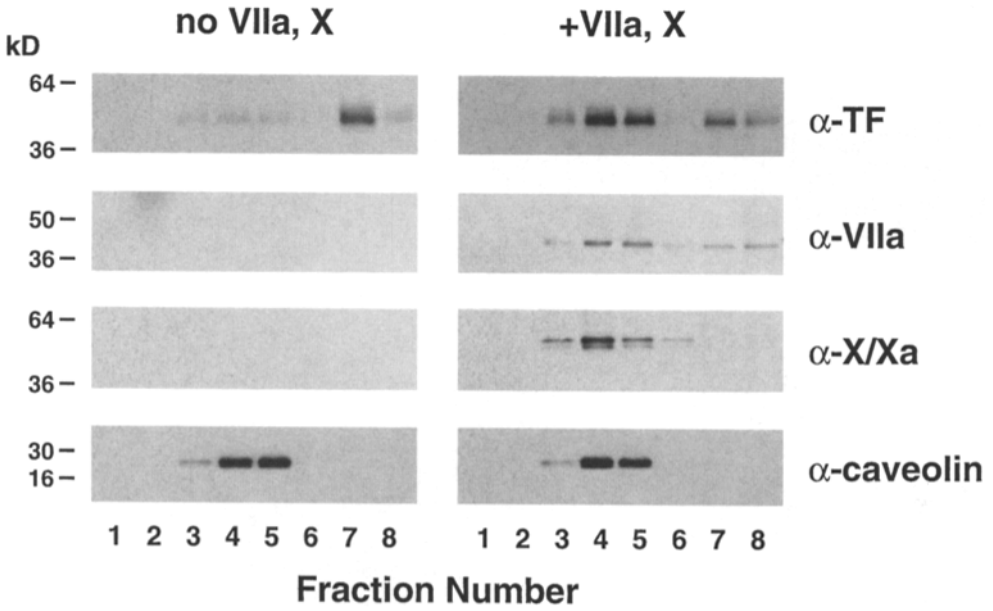

Figure 3. Translocation of TF, VIIa, and Xa into low density, detergent-insoluble microdomains. Equal amounts of protein from each fraction were separated on 8–16% SDS-PAGE gradient gels and transferred for Western blotting with polyclonal antibody to TF or mAbs to VIIa, X/Xa, and caveolin. Fractions are labeled from the top of the sucrose gradient; fractions 7 and 8 contain the Triton X-100–soluble material adjusted to 40% sucrose. In the right panel (*+VIIa, X*), the cells had been incubated with VIIa (10 nM) on ice, followed by substrate 200 nM factor X for 15 min at 37°C. The left panel (*no VIIa, X*) shows the control experiment that was incubated under the same conditions in the absence of both VIIa and factor X.

tions. Fig. 5 *a* shows the comparison of sucrose gradient separations of cells that had been incubated with no ligand, VIIa alone, or VIIa in the presence of factor X. There was no difference between the experimental conditions when the recovery of total protein from the gradient fractions was compared. In each case, ~85–90% of the extracted proteins were recovered in fraction 7 and 8, whereas fractions 3, 4, and 5 contained ~3–7% of the total protein in the gradient. A constant amount of protein from each fraction was loaded per lane for the analysis of TF content by Western blotting, and the densitometric quantitation was normalized by an internal standard on each gel (Fig. 5 *b*, *upper panel*). The distribution of the total cellular TF was calculated based on the TF concentration in each lane and the total protein content of each fraction. In the absence of ligand, 97% of TF was detergent soluble in fractions 7 and 8, and <2% was found in the caveolin-rich fractions 3, 4, and 5. Binding of VIIa to TF resulted in translocation of 8% of the total cellular TF from the detergent-soluble to the low density fractions. In the presence of factor X, the TF content in the low density fractions increased to a total of 58% of the total cellular TF, demonstrating a major redistribution of the receptor.

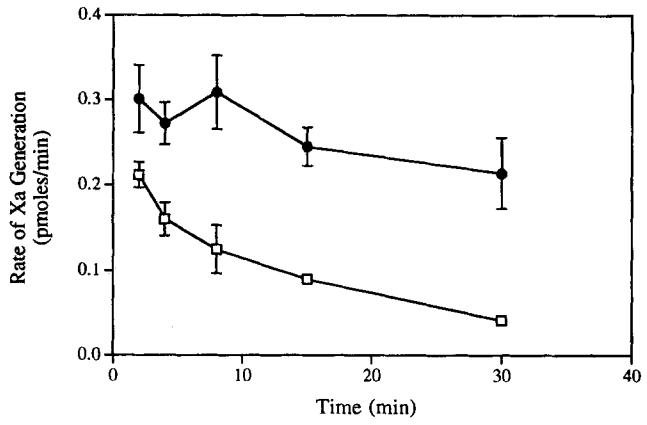

Figure 4. Effect of antibodies to TFPI on the downregulation of TF function. The rate of Xa generation on TNFα-stimulated ECV304 monolayer over time is shown in the absence (□) or presence (●) of 100 μg/ml inhibitory anti-TFPI polyclonal antibody. Mean and SD of triplicate determinations are given.

Fractions of equal total protein concentration were analyzed for TF functional activity. To compensate for potential dissociation of the TF·VIIa complex during the fractionation, excess VIIa was added, and the rate of factor X activation was determined as a measure for TF activity. Control reactions in the presence of high concentrations of a potent inhibitory mAb to TF demonstrated that the activities measured were TF specific and not caused by other unrelated copurifying proteases. The highest TF activity was consistently observed in fraction 7, whereas very low activity was observed in fraction 8 (Fig. 5 *b*, *lower panel*), despite the immunochemical detection of a similar TF content in both fractions (Fig. 5 *b*, *upper panel*). The latter fraction may represent a pool of TF with low proteolytic activity that has been identified on the cell surface (29).

The specific activity of TF in the low density fractions was also significantly lower than TF activity in fraction 7. Moreover, redistribution of TF into low density fractions was not associated with concordant increases of proteolytic function in these fractions. Compared to the control in the absence of ligand, TF content normalized for total protein in fractions 3–5 increased fourfold in the presence of VIIa and 19-fold with both VIIa and factor X present (Fig. 5 *b*, *upper panel*). This resulted in only a two- or threefold increase in TF activity for the same fractions, respectively

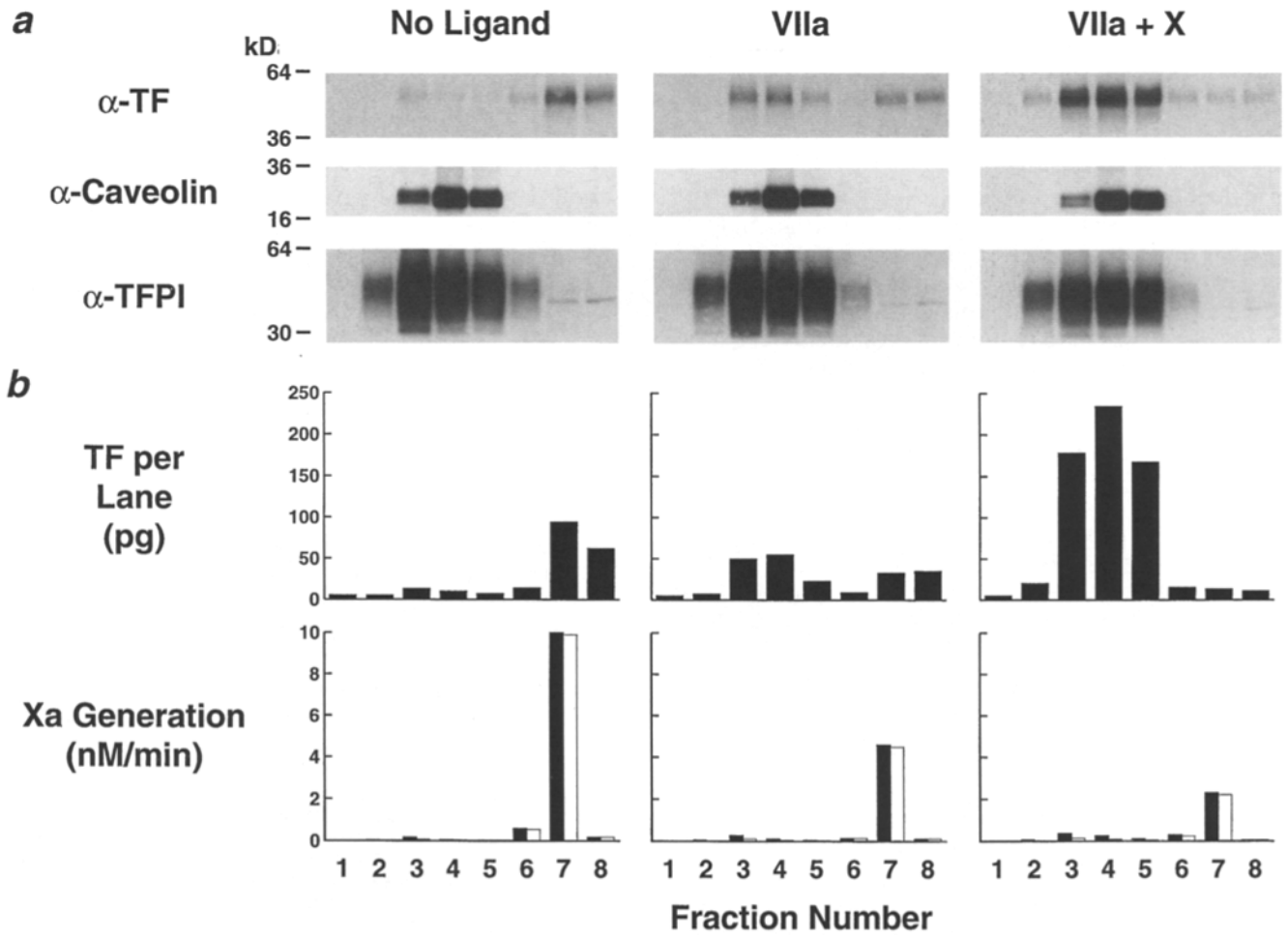

Figure 5. TF functional activity in detergent-soluble and -insoluble fractions. TNFα-stimulated ECV304 cells were lysed with Triton X-100 and fracionated on density gradient after incubation with no ligand, VIIa alone, or VIIa and substrate factor X. (*a*) Western blot analyses of the fractions for TF, caveolin, and TFPI are shown. (*b, upper panel*) TF content per 5 μg of total protein in each fraction was determined by laser densitometry, calibrated by internal standard on the blots; (*lower panel*) the TF functional activity in each fraction (normalized to 2.5 μg/ml total protein) in an experiment representative for four is shown (*open bars*). The marked difference in functional activity between fraction 7 and 8 was further confirmed on six randomly chosen gradient separations. Mixing experiments between fraction 7 and 8 further demonstrated additive functional activities excluding that an inhibitor for TF function accumulated in fraction 8. The functional activity in the gradient fractions was further determined in the presence (*filled bars*) of 50 μg/ml inhibitory antibodies to TFPI that had no effect in fraction 7 and 8 but consistently increased the functional activity in the low density fractions two- to threefold.

(Fig. 5 *b*, *lower panel*). When the fractions were incubated with blocking anti-TFPI antibodies, the activity in the low density fractions increased two- to threefold, but no change in activity was observed in the Triton X-100–soluble fractions (Fig. 5 *b*, *lower panel*). This demonstrates that only TFPI present in low density membrane fractions is contributing to the inhibition of TF function. However, blocking TFPI in the low density fractions did not restore proteolytic function of TF·VIIa to levels comparable to TF in fraction 7, indicating that the glycosphingolipid-rich membrane composition is not favorable for factor X activation and thus independently supports the downregulation of TF·VIIa function.

TFPI Is Localized in Low Density Fractions

The antibody blocking experiments indicated that low-density detergent-insoluble fractions are critical for the inhibition of TF·VIIa by TFPI. Consistently, TFPI was almost exclusively localized in detergent-insoluble fractions under all the experimental conditions tested (Fig. 5 *a*), including cells which were not stimulated by TNFα (not shown). Based on densitometric scans of Western blots, we estimated that >80% of the cellular TFPI was associated with fractions 3–5 (Fig. 5 *a*). Although heterogeneous, a significant portion of the detected TFPI was >43 kD, indicative of full-length TFPI with an intact third Kunitz-type domain and possibly the basic carboxyl terminus, both of which have been implicated in binding to cell surfaces (15, 66). A minor band of lower molecular weight immunoreactive material was usually detected in the Triton X-100–soluble material. This may represent carboxyl-terminal truncated TFPI in the degradative pathway that is mediated by the low density lipoprotein (LDL) receptor–related protein (65). The almost exclusive presence of TFPI in Triton X-100–insoluble complexes is consistent

with a mechanism of inhibition of TF·VIIa function through stable quaternary complex formation in a glycosphingolipid-rich microenvironment on cells.

GPI-linked Binding Sites for TFPI Are Responsible for Partitioning in Low Density Fractions

The method for preparation of detergent-insoluble fractions can be considered reliable for the localization of proteins to low density microdomains, if the protein is expressed on external membranes, as in the case of TF. Since the binding sites for TFPI are not defined, one needs to consider a predominant localization of the inhibitor in internal membranes that are known to show similar partitioning into low density fractions (27). To address this possibility, we used the protease sensitivity of TFPI to distinguish between external and intracellular pools. We determined by ELISA that ECV304 cells have 26 ± 5 ng TFPI per 10^7 cells, corresponding to 52,000 ± 10,000 molecules/cell (n = 3). By functional assay, we concordantly determined 26 ± 6 ng TFPI per 10^7 cells (n = 4), and from densitometric analysis, we estimate ~120,000 molecules per cell, slightly less than the concentration of TF on stimulated ECV304. When intact ECV304 cells (>90% viable) were incubated on ice with either proteinase K or chymotrypsin, cell-associated TFPI determined by ELISA was reduced by >90% (<2.4 ng/10^7 cells, below the calibration range of the ELISA). From these data we conclude that TFPI is almost entirely localized on external membranes.

The almost exclusive partitioning of TFPI into low density microdomains suggested a specific binding site with localization to a restricted glycosphingolipid environment on the cell surface. GPI-linked proteins are known to partition in detergent-insoluble microdomains (39), and we considered the possibility that TFPI is selectively bound to GPI-linked sites on endothelial cells. GPI-linked proteins further partition into the detergent phase, when temperature-induced phase separation with Triton X-114 is used to fractionate cells. Fig. 6 demonstrates the recovery of TFPI in the detergent phase of a Triton X-114 lysate of ECV304 cells. Protease treatment virtually removed all TFPI when proteinase K and chymotrypsin were used, and elastase significantly reduced the higher molecular weight form of TFPI. Enzymatic cleavage of the GPI anchor with phosphatidylinositol-specific phospholipase C further substantially reduced TFPI partitioning into the detergent phase of Triton X-114. These data suggest that the as yet to be defined receptor for TFPI is GPI linked and localized in the glycosphingolipid-rich parts of the external membranes. We could not identify antibodies directed to TFPI, VIIa, or factor X that are reactive with the proteins after formation of the quaternary complex. Ultrastructural analysis, as performed for TF, could therefore not be used to substantiate that each of the reactants in the quaternary complex translocate into caveolae, as defined by ultrastructural morphology.

Requirements for the Translocation of TF into Triton X-100–insoluble Domains

We used the change in detergent solubility of TF to characterize the critical interactions that allow translocation of the receptor TF into low density glycosphingolipid-rich microdomains (Fig. 7). The binding of ligand VIIa increased TF detergent insolubility only slightly, consistent with the reported low affinity for complex formation of TF·VIIa with TFPI (7) that is thought to involve the first Kunitz-type domain (20). The addition of factor X or 5 nM Xa, which is approximatley the concentration of Xa generated during a 5–10-min reaction, effectively promoted translocation into low density fractions (Fig. 7). Regardless whether factor X or Xa was added, Xa was detected, suggesting that the generation of product Xa is critical for the translocation into the detergent-insoluble fractions. Although 5 nM Xa promoted the translocation of the TF·VIIa complex, no change in detergent solubility was observed when the same concentration of Xa was added in the absence of VIIa (Fig. 7). These data suggest that the proposed complex formation of Xa with TF alone, which was inferred from in vitro experiments with purified components (18), does not support the translocation of TF and the cellular inhibition of function.

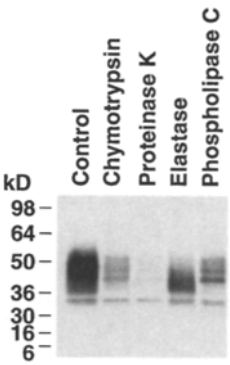

Figure 6. Triton X-114 extraction of TFPI and release of cell surface TFPI by proteases and phospholipase C. The Triton X-114 extract of 5×10^5 cells is loaded per lane, and TFPI is detected by Western blotting using polyclonal anti-TFPI antibody. Suspensions of intact cells were treated at 4°C with 500 μg/ml of the indicated protease or at 37°C with 0.5 U of phosphatidylinositol-specific phospholipase C before extraction with Triton X-114.

The concentration of Xa in the detergent-insoluble fractions was fourfold lower in the absence of VIIa, as compared to the experiment in which TF·VIIa translocation was observed (Fig. 7). These data indicate that translocation of the TF·VIIa complex increases the concentration of Xa in the detergent-insoluble fractions, possibly through a transient ternary complex formation of TF·VIIa with Xa preceding the translocation event. When TFPI is blocked by antibody, only traces of Xa are detected in the detergent-insoluble fractions, and TF translocation is prevented. The stable localization of TF in the different membrane environment must then be dependent on the assembly of factor Xa with TFPI. Consistently, preventing the assembly of Xa with TFPI by covalent active site inhibition of Xa with glutamyl-glycyl-arginyl-chloromethyl ketone (EGR-Xa) abolished translocation. The presented data are consistent with a central role of the product protease Xa in mediating quaternary complex formation in detergent-insoluble microdomains achieving downregulation of the TF·VIIa complex through translocation of the receptor TF.

Discussion

This study analyzes the regulation of cell surface assembly of the coagulation cascade that is triggered by the protease receptor TF. We find that TF redistributes into caveolae upon binding of VIIa and generation of product Xa, based on the following experimental approaches. First, TF in the

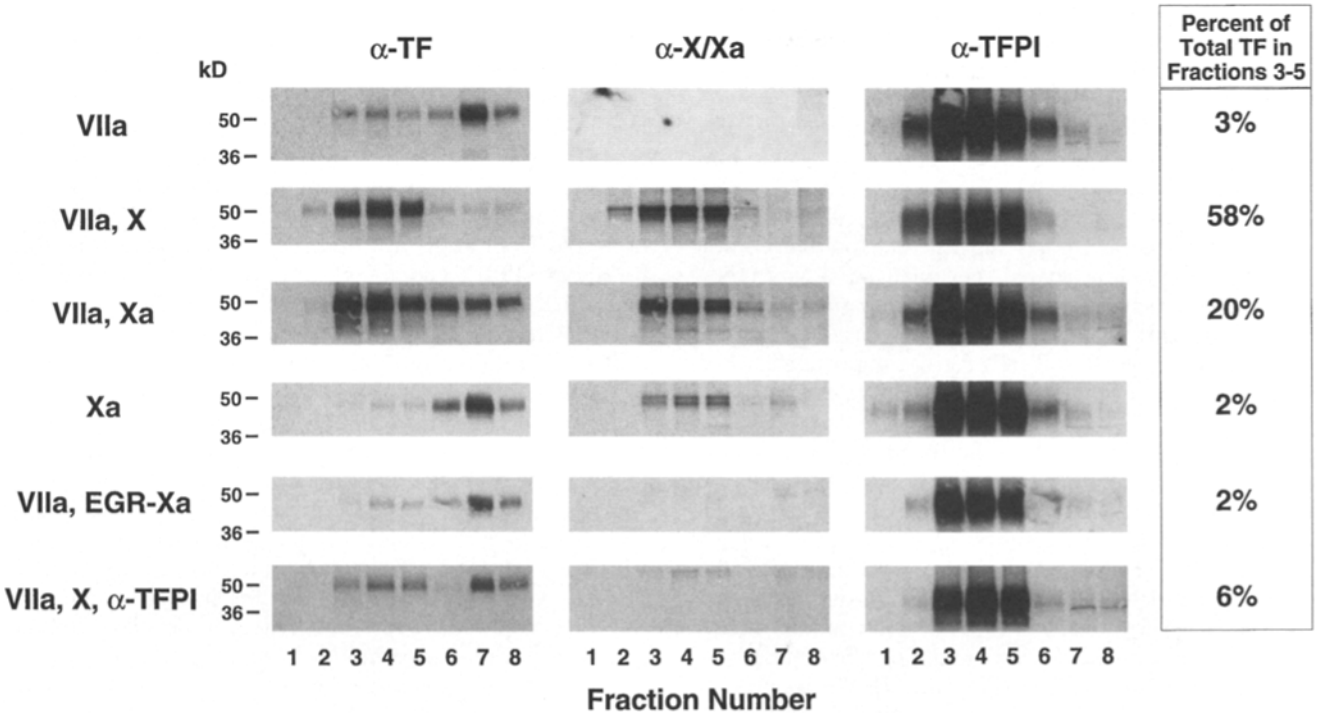

Figure 7. Requirements for the redistribution of TF into caveolin-rich microdomains. Western blot analysis for TF, factor X/Xa, and TFPI of density gradient fractionations of ECV304. Cells were incubated with VIIa where indicated for 1 h at 4°C, followed by a 15-min reaction at 37°C with buffer, 200 nM factor X (*X*), 5 nM Xa (*Xa*), or 5 nM Xa inhibited at the active site with glutamyl-glycyl-arginyl-chloromethyl ketone (*EGR-Xa*). Inhibitory polyclonal antibodies to TFPI (*α-TFPI*) were included with 200 nM factor X (*X*) at a concentration of 30 μg/ml. TF content was determined from densitometric scanning of the blots that had equal amounts of protein loaded. Based on the total protein in each fraction, the TF distribution was calculated and shown as the percentage that partitions into fraction 3–5.

presence of VIIa and factor X was localized to plasmalemma vesicles by immunogold EM. This contrasts with the analysis in the absence of ligands that demonstrates predominant localization of TF on the cell membrane and on cellular processes, as previously described for TF (12, 22, 34). The lack of significant TF staining in caveolae in the absence of ligand excludes that antibody-dependent nonspecific clustering into caveolae (32) is induced by the experimental conditions. We observe a ninefold increase of TF in plasmalemma vesicles after a 15-min incubation of the TF·VIIa complex with substrate factor X. These vesicles have the typical shape and size (60–100 nm) of caveolae.

Second, we observe a ligand-dependent change in Triton X-100 solubility of the transmembrane receptor, resulting in association of TF with caveolin-rich low density fractions after separation by sucrose gradient ultracentrifugation. Formation of the complex of TF with the ligand protease VIIa changed Triton X-100 solubility only slightly, but a 10-fold increase of TF in the detergent-insoluble fractions was observed after a 15-min incubation of the TF·VIIa complex with the substrate factor X. As much as 60% of the total cellular TF redistributed from the detergent-soluble fractions to the low density fractions enriched in caveolin. Thus, independent lines of evidence support receptor translocation into caveolae as a consequence of activation of the substrate factor X.

The translocation of TF is associated with downregulation of TF·VIIa proteolytic function. Antibody blocking experiments demonstrated that the inhibition of function is mediated by the major inhibitor of the TF pathway, the Kunitz-type inhibitor TFPI. TFPI was detected mostly (>80%) in Triton X-100–insoluble fractions after density gradient separation. TFPI is a secreted protein and can bind to undefined receptors that are inferred from circumstantial evidence to be heparan sulfate proteoglycans or glycosaminoglycans on endothelial cells (53). The predominant localization of TFPI in low density fractions indicates that the putative binding sites for TFPI on endothelial cells have a restricted distribution. TFPI can be internalized through the α_2-macroglobulin receptor/LDL receptor–related protein mediated targeting to clathrin-coated pits in hepatoma cells (65). The internalization and degradation through the LDL receptor–related protein is inhibited by the receptor-associated protein (RAP), but RAP blocks only a small percentage of the binding of TFPI to hepatoma cells (36). When internalized through the clathrin-coated pits pathway, TFPI should remain Triton X-100 soluble and, based on the almost complete detergent insolubility, we thus exclude a stable association of a significant portion of the cellular TFPI to the LDL receptor–related protein on endothelial cells.

We show that the predominant binding sites for TFPI on endothelial cells are on external membranes and GPI linked. The recovery of GPI-linked proteins in detergent-insoluble fractions is a consequence of the association of the glycolipid anchor with microdomains that are enriched in sphingolipids and cholesterol (5, 24, 54, 57). GPI-linked proteins have further been shown to be associated with cav-

eolae prepared in the absence of detergent (59), providing evidence that the partitioning is not simply an artifact of detergent solubilization. GPI-linked proteins partition into low density fractions prepared from cells that are devoid of caveolae (16, 21), demonstrating that the coat provided by caveolin is not required to constitute glycosphingolipid-rich microdomains on the cell membrane. Caveolae share the specific lipid composition with these microdomains, and several studies suggest that the distribution of GPI-linked proteins between caveolae and adjacent glycosphingolipid-rich microdomains is dynamically regulated (32, 40, 56). The ultrastructural localization of the binding sites for TFPI will be of great importance when the receptor will be identified and suitable reagents become available.

Inhibition by TFPI involves the formation of a quaternary complex with TF, VIIa, and Xa. In addition to TF, we find that the ligand protease VIIa, as well as the product Xa, change detergent solubility, providing evidence for quaternary TF·VIIa·Xa·TFPI complex formation in glycosphingolipid-rich microdomains. TFPI in the absence of Xa has been shown to inhibit the TF·VIIa complex, based on analyses with purified components or when added exogenously to cells expressing TF·VIIa (7). We found that the TF content in the Triton X-100–insoluble fractions increased only two- to fourfold in the presence of VIIa alone, whereas 10- to 20-fold increases were observed when factor X was present with the TF·VIIa complex. This suggests that the inhibition of TF·VIIa by cell-associated TFPI is inefficient in the absence of Xa. The finding also indicates that the Ca^{2+} flux in response to VIIa binding to TF (45) is not the driving force for redistribution of TF into low density microdomains and caveolae.

Presence of the substrate factor X or the product Xa effectively promoted the change in detergent solubility of TF·VIIa, suggesting that not substrate interaction per se, but rather the generation of Xa, is essential for the redistribution of TF. Blocking TFPI–Xa interaction by occupancy of the catalytic site of Xa with a covalent peptidyl inhibitor or by inhibitory anti-TFPI antibodies prevented the redistribution of TF into low density fractions. TF in the presence of Xa, but absence of VIIa, changed detergent solubility insignificantly, demonstrating that the stable assembly with TFPI requires the enzyme VIIa bound to TF. These data emphasize that each of the reactants that form the quaternary TF·VIIa·Xa·TFPI complex is required for stable localization in low density microdomains. Notably, in the absence of VIIa, substantially less Xa is bound to TFPI in the low density fractions, indicating that no stable TFPI·Xa complex is preformed for the assembly with TF·VIIa. These data suggest that a transient complex of TF·VIIa with Xa facilitates translocation and association with TFPI in glycosphingolipid-rich microdomains.

Based on the presented data, we suggest the following sequence of events in the downregulation of TF·VIIa function on endothelial cells (Fig. 8). The TF·VIIa complex has the highest functional activity in an anionic environment of the plasma membrane. Transient assembly with Xa greatly facilitates the interaction of the complex with the inhibitor TFPI that is bound to a GPI-linked molecule localized in glycosphingolipid-rich microdomains of the external plasma membrane. One can speculate that the quaternary complex assembles in caveolae or, as depicted in Fig. 8, that the macromolecular assembly in noncaveolar glycosphingolipid-rich microdomains triggers translocation of the inhibited complex into caveolae. Although the presented data cannot exclude that the quaternary complex dissociates before the ultrastructurally observed translocation of TF into caveolae, this is considered likely only as a secondary and slow process, because of the tight binding of the inhibitor in the presence of Xa (23).

Based on this study, caveolae are implicated in the regulation of cell surface proteolysis. This concept is also supported by the observation that the urokinase receptor is localized in caveolae of tumor cells (60). The constitutive targeting of the urokinase receptor to caveolae, possibly a consequence of its GPI anchor (5), imparts to caveolae the ability to promote urokinase receptor–dependent plasminogen activation leading to pericellular plasmin generation and fibrinolysis. We observed that the specific activity of

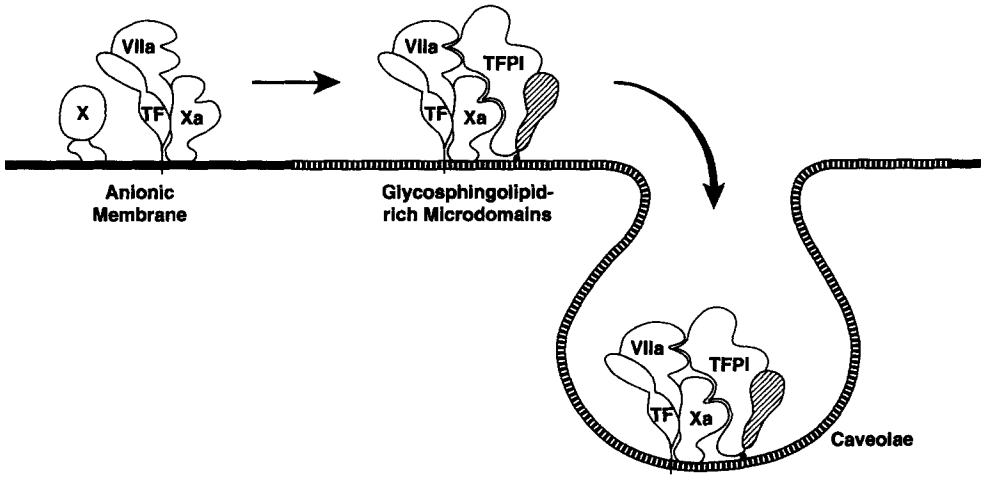

Figure 8. Schematic model for the assembly of the TF·VIIa complex with TFPI on cells. The activation of factor X is accelerated by binding of the substrate to anionic sites on the cell membrane and the generation of Xa supports binding of TFPI to TF·VIIa. TFPI is associated with GPI-linked binding sites that are located in glycosphingolipid-rich microdomains. Assembly of TF·VIIa·Xa with TFPI may occur in caveolae or involve a two-step process in which the quaternary complex forms in microdomains followed by translocation of complex into caveolae, as indicated in the figure.

TF was higher in Triton X-100–soluble fractions than in the low density fractions, even in the presence of inhibitory antibodies to TFPI. The decreased specific activity of TF in the glycosphingolipid-enriched microdomains may, in part, result from direct inhibition by sphingolipids that have been shown to interfere with enzyme binding to TF (10). Plasmalemma vesicles notably lack anionic binding sites (58) to which substrates factor X and IX can bind via their charged amino-termianl γ-carboxyglutamic acid–rich domains. Membrane binding of substrate greatly enhances activation by TF·VIIa (26, 51). Hence, TF function will be suppressed by the lack of anionic binding sites for substrate in caveolae. Translocation of TF into caveolae and expression of urokinase receptor–dependent plasmin generation in caveolae thus result in the concordant effect of diminishing pericellular fibrin formation by reducing the procoagulant activity while supporting fibrinolysis.

Certain G protein–coupled receptors have been shown to localize to caveolae after ligand interaction (9, 42, 43), and the subsequent internalization through caveolae has been proposed as a mechanism for downregulation of receptor function (42, 43). Inhibitors that block the internalization of alkaline phosphatase into caveolae (40) did not affect the downregulation of TF·VIIa complex function (not shown). This suggests that internalization of TF through a caveolae-dependent pathway is not essential for assembly with TFPI and the inhibition of function. Caveolin has further been demonstrated to interact with Gα-subunits in their inactive, GDP-bound form (30), suggesting that receptor translocation into caveolae downregulates signaling through G protein–coupled receptors. It is unclear what triggers the translocation of these receptors into caveolae, but one may consider the assembly of signaling molecules on the cytoplasmic side of the membrane. Our study indicates that extracellular macromolecular assemblies also represent an adequate trigger for the redistribution of receptors into caveolae, providing receptor sequestration and downregulation of function.

We thank Pablito Tejada for invaluable technical assistance and Dr. Cheng-Ming Chang for performing the EM. We thank Dr. Sandra L. Schmid for critical advice and Tom Edgington for support and discussion throughout these studies.

This work was supported by National Institutes of Health grants HL-16411 (to W. Ruf) and HL-42813 (to L.V.M. Rao).

Received for publication 21 August 1995 and in revised form 7 February 1996.

References

1. Ameri, A., M.N. Kuppuswamy, S. Basu, and S.P. Bajaj. 1992. Expression of tissue factor pathway inhibitor by cultured endothelial cells in response to inflammatory mediators. *Blood.* 79:3219–3226.
2. Anderson, R. 1993. Caveolae: where incoming and outgoing messengers meet. *Proc. Natl. Acad. Sci. USA.* 90:10909–10913.
3. Behrendt, N., E. Ronne, M. Ploug, T. Petri, D. Lober, L.S. Nielsen, W.-D. Schleuning, F. Blasi, E. Appella, and K. Dano. 1990. The human receptor for urokinase plasminogen activator. *J. Biol. Chem.* 265:6453–6460.
4. Bom, V.J.J., V.W.M. Van Hinsbergh, H.H. Reinalda-Poot, R.W. Mohanlal, and R.M. Bertina. 1991. Extrinsic activation of human coagulation factors IX and X on the endothelial surface. *Thromb. Haemostasis.* 66:283–291.
5. Brown, D.A., and J.K. Rose. 1992. Sorting of GPI-anchored proteins to glycolipid-enriched membrane subdomains during transport to the apical cell surface. *Cell.* 68:533–544.
6. Broze, G.J., Jr., T.J. Girard, and W.F. Novotny. 1990. Regulation of coagulation by a multivalent Kunitz-type inhibitor. *Biochemistry.* 29:7539–7546.
7. Callander, N.S., L.V.M. Rao, O. Nordfang, P.M. Sandset, B. Warn-Cramer, and S.I. Rapaport. 1992. Mechanisms of binding of recombinant extrinsic pathway inhibitor (rEPI) to cultured cell surfaces. Evidence that rEPI can bind to and inhibit factor VIIa-tissue factor complexes in the absence of factor Xa. *J. Biol. Chem.* 267:876–882.
8. Carson, S.D., G.A. Perry, and S.J. Pirruccello. 1994. Fibroblast tissue factor: calcium and ionophore induce shape changes, release of membrane vesicles, and redistribution of tissue factor antigen in addition to increased procoagulant activity. *Blood.* 84:526–534.
9. Chun, M., U.K. Liyanage, M.P. Lisanti, and H.F. Lodish. 1994. Signal transduction of a G protein-coupled receptor in caveolae: colocalization of endothelin and its receptor with caveolin. *Proc. Natl. Acad. Sci. USA.* 91: 11728–11732.
10. Conkling, P.R., K.L. Patton, Y.A. Hannun, C.S. Greenberg, and J.B. Weinberg. 1989. Sphingosine inhibits monocyte tissue factor-initiated coagulation by altering factor VII binding. *J. Biol. Chem.* 264:18440–18444.
11. Contrino, J., G. Hair, M. Schmeizl, F. Rickles, and D. Kreutzer. 1994. In situ characterization of antigenic and functional tissue factor expression in human tumors utilizing monoclonal antibodies and recombinant factor VIIa as probes. *Am. J. Pathol.* 145:1315–1322.
12. Drake, T.A., W. Ruf, J.H. Morrissey, and T.S. Edgington. 1989. Functional tissue factor is entirely cell surface expressed on lipopolysaccharide-stimulated human blood monocytes and a constitutively tissue factor–producing neoplastic cell line. *J. Cell Biol.* 109:389–395.
13. Drake, T.A., J. Cheng, A. Chang, and F.B. Taylor, Jr. 1993. Expression of tissue factor, thrombomodulin, and E-selectin in baboons with lethal *E. coli* sepsis. *Am. J. Pathol.* 142:1458–1470.
14. Ellis, V., C. Pyke, J. Erikson, H. Solberg, and K. Dano. 1992. The urokinase receptor: involvement in cell surface proteolysis and cancer invasion. *Ann. NY Acad. Sci.* 667:13–31.
15. Enjyoji, K., T. Miyata, Y. Kamikubo, and H. Kato. 1995. Effect of heparin on the inhibition of factor Xa by tissue factor pathway inhibitor: a segment, Gly^{212}-Phe^{243}, of the third Kunitz domain is a heparin-binding site. *Biochemistry.* 34:5725–5735.
16. Fra, A., E. Williamson, K. Simons, and R. Parton. 1994. Detergent-insoluble glycolipid microdomains in lymphocytes in the absence of caveolae. *J. Biol. Chem.* 269:30745–30748.
17. Fujimoto, T., S. Nakade, A. Miyawaki, K. Mikoshiba, and K. Ogawa. 1992. Localization of inositol 1,4,5-trisphosphate receptor-like protein in plasmalemmal caveolae. *J. Cell Biol.* 119:1507–1513.
18. Gemmell, C.H., G.J. Broze, Jr., V.T. Turitto, and Y. Nemerson. 1990. Utilization of a continuous flow reactor to study the lipoprotein-associated coagulation inhibitor (LACI) that inhibits tissue factor. *Blood.* 76:2266–2271.
19. Geoghegan, W.D., and G.A. Ackerman. 1977. Adsorption of horseradish peroxidase, ovomucoid and anti-immunoglobulin to colloidal gold for the indirect detection of concanavalin A, wheat germ agglutinin and goat anti-human immunoglobulin G on cell surfaces at electron microscopic level: a new method, theory and application. *J. Histochem. Cytochem.* 25: 1187–1200.
20. Girard, T.J., L.A. Warren, W.F. Novotny, K.M. Likert, S.G. Brown, J.P. Miletich, and G.J. Broze, Jr. 1989. Functional significance of the Kunitz-type inhibitory domains of lipoprotein-associated coagulation inhibitor. *Nature (Lond.).* 338:515–520.
21. Gorodinsky, A., and D.A. Harris. 1995. Glycolipid-anchored proteins in neuroblastoma cells form detergent-resistant complexes without caveolin. *J. Cell Biol.* 129:619–627.
22. Gupta, M., G.J. Doellgast, T. Cheng, and J.C. Lewis. 1993. Expression and localization of tissue factor-based procoagulant activity (PCA) in pigeon monocyte-derived macrophages. *Thromb. Haemostasis.* 70:963–969.
23. Hamamoto, T., M. Yamamoto, O. Nordfang, J.G.L. Petersen, D.C. Foster, and W. Kisiel. 1993. Inhibitory properties of full-length and truncated recombinant tissue factor pathway inhibitor (TFPI): evidence that the third Kunitz-type domain of TFPI is not essential for the inhibition of factor VIIa-tissue factor complexes on cell surfaces. *J. Biol. Chem.* 268:8704–8710.
24. Hanada, K., M. Nishijima, Y. Akamatsu, and R.E. Pagano. 1995. Both sphingolipids and cholesterol participate in the detergent insolubility of alkaline phosphatase, a glycosylphosphatidylinositol-anchored protein, in mammalian membranes. *J. Biol. Chem.* 270:6254–6260.
25. Kirchhofer, D., T.B. Tschopp, P. Hadváry, and H.R. Baumgartner. 1994. Endothelial cells stimulated with tumor necrosis factor-α express varying amounts of tissue factor resulting in inhomogeneous fibrin deposition in a native blood flow system. *J. Clin. Invest.* 93:2073–2083.
26. Krishnaswamy, S., K.A. Field, T.S. Edgington, J.H. Morrissey, and K.G. Mann. 1992. Role of the membrane surface in the activation of human coagulation factor X. *J. Biol. Chem.* 267:26110–26120.
27. Kurzchalia, T.V., P. Dupree, and S. Monier. 1994. VIP21-caveolin, a protein of the *trans*-Golgi network and caveolae. *FEBS Lett.* 346:88–91.
28. Kyhse-Anderson, J. 1984. Electroblotting of multiple gels: a simple apparatus without buffer tank for rapid transfer of proteins from polyacrylamide to nitrocellulose. *J. Biochem. Biophys. Methods.* 10:203–209.
29. Le, D.T., S.I. Rapaport, and L.V.M. Rao. 1992. Relations between factor VIIa binding and expression of factor VIIa/tissue factor catalytic activity on cell surfaces. *J. Biol. Chem.* 267:15447–15454.

30. Li, S., T. Okamoto, M. Chun, M. Sargiacomo, J. Casanova, S. Hansen, I. Nishimoto, and M. Lisanti. 1995. Evidence for a regulated interaction between heterotrimeric G proteins and caveolin. *J. Biol. Chem.* 270:15693–15701.
31. Lisanti, M., P. Scherer, J. Vidugiriene, Z. Tang, A. Hermanowski-Vosatka, Y.-H. Tu, R.F. Cook, and M. Sargiacomo. 1994. Characterization of caveolin-rich membrane domains isolated from an endothelial-rich source: implications for human disease. *J. Cell Biol.* 126:111–126.
32. Mayor, S., K. Rothberg, and F. Maxfield. 1994. Sequestration of GPI-anchored proteins in caveolae triggered by cross-linking. *Science (Wash. DC).* 264:1948–1951.
33. Mulder, A.B., K.S.M. Hegge-Paping, C.P.E. Magielse, N.R. Blom, J.W. Smit, J. van der Meer, M.R. Halie, and V.J.J. Bom. 1994. Tumor necrosis factor α-induced endothelial tissue factor is located on the cell surface rather than in the subendothelial matrix. *Blood.* 84:1559–1566.
34. Müller, M., C. Flössel, M. Haase, T. Luther, S. Albrecht, P.P. Nawroth, and Y. Zhang. 1993. Cellular localization of tissue factor in human breast cancer cell lines. *Virchows Arch. B. Cell Pathol.* 64:265–269.
35. Narahara, N., T. Enden, M. Wiiger, and H. Prydz. 1994. Polar expression of tissue factor in human umbilical vein endothelial cells. *Arterioscler. Thromb.* 14:1815–1820.
36. Narita, M., G. Bu, G.M. Olins, D.A. Higuchi, J. Herz, G.J. Broze, Jr., and A.L. Schwartz. 1995. Two receptor systems are involved in the plasma clearance of tissue factor pathway inhibitor *in vivo*. *J. Biol. Chem.* 270: 24800–24804.
37. Nawroth, P.P., and D.M. Stern. 1986. Modulation of endothelial hemostatic properties by tumor necrosis factor. *J. Exp. Med.* 163:740–745.
38. Palade, G.E., and R.R. Bruns. 1968. Structural modulation of plasmalemma vesicles. *J. Cell Biol.* 37:633–649.
39. Parton, R.G., and K. Simons. 1995. Digging into caveolae. *Science (Wash. DC).* 269:1398–1399.
40. Parton, R., B. Joggerst, and K. Simons. 1994. Regulated internalization of caveolae. *J. Cell Biol.* 127:1199–1215.
41. Rapaport, S.I., and L.V.M. Rao. 1995. The tissue factor pathway: how it has become a "Prima Ballerina." *Thromb. Haemostasis.* 74:7–17.
42. Raposo, G., I. Dunia, S. Marullo, C. Andre, J. Guillet, A.D. Strosberg, E. Benedetti, and J. Hoebeke. 1987. Redistribution of muscarinic acetylcholine receptors on human fibroblasts induced by regulatory ligands. *Biol. Cell.* 60:117–124.
43. Raposo, G., I. Dunia, C. Delavier-Klutchko, S. Kaveri, A.D. Strosberg, and E.L. Benedetti. 1989. Internalization of β-adrenergic receptor in A431 cells involves non-coated vesicles. *Eur. J. Cell Biol.* 50:340–352.
44. Rothberg, K., J. Heuser, W. Donzell, Y. Ying, J. Glenney, and R. Anderson. 1992. Caveolin, a protein component of caveolae membrane coats. *Cell.* 68:673–682.
45. Rottingen, J.A., T. Enden, E. Camerer, J. Iversen, and H. Prydz. 1995. Binding of human factor VIIa to tissue factor induces cytosolic Ca2+ signals in J82 cells, transfected COS-1 cells, MDCK cells and in human endothelial cells induced to synthesize tissue factor. *J. Biol. Chem.* 270: 4650–4660.
46. Ruf, W. 1994. Factor VIIa residue Arg^{290} is required for efficient activation of the macromolecular substrate factor X. *Biochemistry.* 33:11631–11636.
47. Ruf, W., and T.S. Edgington. 1991. An anti-tissue factor monoclonal antibody which inhibits TF:VIIa complex is a potent anticoagulant in plasma. *Thromb. Haemostasis.* 66:529–533.
48. Ruf, W., and T.S. Edgington. 1994. Structural biology of tissue factor, the initiator of thrombogenesis in vivo. *FASEB (Fed. Am. Soc. Exp. Biol.) J.* 8:385–390.
49. Ruf, W., A. Rehemtulla, J.H. Morrissey, and T.S. Edgington. 1991. Phospholipid independent and dependent interactions required for tissue factor receptor and cofactor function. *J. Biol. Chem.* 266:2158–2166.
50. Ruf, W., A. Rehemtulla, and T.S. Edgington. 1991. Antibody mapping of tissue factor implicates two different exon-encoded regions in function. *Biochem. J.* 278:729–733.
51. Ruf, W., E.A. Stura, R.J. LaPolla, R. Syed, T.S. Edgington, and I.A. Wilson. 1992. Purification, sequence and crystallization of an anti-tissue factor Fab and its use for the crystallization of tissue factor. *J. Cryst. Growth.* 122:253–264.
52. Ruf, W., D.J. Miles, A. Rehemtulla, and T.S. Edgington. 1993. Mutational analysis of receptor and cofactor function of tissue factor. *Methods Enzymol.* 222:209–224.
53. Sandset, P.M., U. Abildgaard, and M.L. Larsen. 1988. Heparin induces release of extrinsic coagulation pathway inhibitor (EPI). *Thromb. Res.* 50: 803–813.
54. Sargiacomo, M., M. Sudol, Z. Tang, and M.L. Lisanti. 1993. Signal transducing molecules and glycosyl-phosphatidylinositol-linked proteins form a caveolin-rich insoluble complex in MDCK cells. *J. Cell Biol.* 122:789–807.
55. Schnitzer, J., P. Oh, E. Pinney, and J. Allard. 1994. Filipin-sensitive caveolae-mediated transport in endothelium: reduced transcytosis, scavenger endocytosis, and capillary permeability of select macromolecules. *J. Cell Biol.* 127:1217–1232.
56. Schnitzer, J.E., D.P. McIntosh, A.M. Dvorak, J. Liu, and P. Oh. 1995. Separation of caveolae from associated microdomains of GPI-anchored proteins. *Science (Wash. DC).* 269:1435–1439.
57. Schroeder, R., E. London, and D. Brown. 1994. Interactions between saturated acyl chains confer detergent resistance on lipids and glycosylphosphatidylinositol (GPI)-anchored proteins: GPI-anchored proteins in liposomes and cells show similar behavior. *Proc. Natl. Acad. Sci. USA.* 91: 12130–12134.
58. Simonescu, M., N. Simonescu, and G.E. Palade. 1982. Preferential distribution of anionic sites on the basement membrane and the abluminal aspect of the endothelium in fenestrated capillaries. *J. Cell Biol.* 95:425–434.
59. Smart, E.J., Y.S. Ying, C. Mineo, and R.G.W. Anderson. 1995. A detergent-free method for purifying caveolae membrane from tissue culture cells. *Proc. Natl. Acad. Sci. USA.* 92:10104–10108.
60. Stahl, A., and B.M. Mueller. 1995. The urokinase-type plasminogen activator receptor, a GPI-linked protein, is localized in caveolae. *J. Cell Biol.* 129:335–344.
61. Takahasi, K., and Y. Sawasaki. 1992. Rare spontaneously transformed human endothelial cell line provides useful research tool. *In Vitro Cell. & Dev. Biol.* 28A:380–382.
62. Tschopp, J., E.R. Podack, and H.J. Müller-Eberhard. 1982. Ultrastructure of the membrane attack complex of complement: detection of the tetramolecular C9-polymerizing complex C5b-8. *Proc. Natl. Acad. Sci. USA.* 79:7474–7478.
63. Vu, T.-K.H., D.T. Hung, V.I. Wheaton, and S.R. Coughlin. 1991. Molecular cloning of a functional thrombin receptor reveals a novel proteolytic mechanism of receptor activation. *Cell.* 64:1057–1068.
64. Warn-Cramer, B.J., and S.L. Maki. 1992. Purification of tissue factor pathway inhibitor (TFPI) from rabbit plasma and characterization of its differences from TFPI isolated from human plasma. *Thromb. Res.* 67:367–383.
65. Warshawsky, I., G.J. Broze, and A.L. Schwartz. 1994. The low density lipoprotein receptor-related protein mediates the cellular degradation of tissue factor pathway inhibitor. *Proc. Natl. Acad. Sci. USA.* 91:6664–6668.
66. Wesselschmidt, R., K. Likert, Z. Huang, L. MacPhail, and G.J. Broze Jr. 1993. Structural requirements for tissue factor pathway inhibitor interactions with factor Xa and heparin. *Blood Coagul. & Fibrinolysis.* 4:661–669.